Physical factors that define the preciseness required in our original, semiconductor-laser cavity scheme for generating 5-picosecond, 40-GHz, optical clock pulses

Hiroyuki Takeuchi, Ryoichi Nakamoto (a), Jun Sakaguchi (b), Takashi Ohira (c), and Yoshiyasu Ueno

University of Electro-Communications (UEC), Department of Electronic Engineering
1-5-1 Chofugaoka, Chofu, Tokyo, 182-8585 Japan
Tel: +81-42-443-5207, e-mail: takeuchi@ultrafast.ee.uec.ac.jp

(a) Present address: Sumitomo Electric Industries, Ltd., Osaka, Japan.
(b) Present address: Nara Institute of Science and Technology (NAIST), Nara, Japan.
(c) Present address: Fujitsu Access, Ltd., Kawasaki, Japan.

Abstract

We had proposed and demonstrated a new scheme of ultrafast, ultrahigh-frequency, 1.55-µm-wavelength, III-V-semiconductor-based optical-clock-pulse generators, which will have significant advantages in monolithically integrating in semiconductor chips, and therefore will play important roles in the fast-growing optical-network systems. In this work, we paid the first attention to the preciseness requirement in terms of the laser-cavity's adjustment. We built an analytical model from the required preciseness viewpoint, and then its validity was successfully verified with systematically measured results using two types of our proto-type laser cavities (i.e., 5-ps, 40-GHz cavity and 5-ps, 10-GHz cavity). The required preciseness, in terms of one internal polarization-controller's axis angle, has turned out to be ±3 to ±5 degrees, for example. The physical factors that define the preciseness requirement have been analytically derived from the above new model, as well, which will be very valuable findings for developing more advanced, sub-picosecond, over-100-GHz-repetition optical-clock-generator designs without requesting too much preciseness in its cavity's structure and for developing its volume-production-level nano-fabrication processes.

1. Introduction

The broadband-network's communication demands are increasing rapidly in the world, according to the latest statistics of broadband subscribers in the OECD countries and China,[1-3] for example. In Japan and Korea in the OECD statistics, in particular, the numbers of optical-fiber-LAN subscribers per 100 inhabitants have reached significantly large numbers (about 8-10 subscribers per them in 2007). Thus, it will presently be more important *to* reinforce *the backbone capacity* for satisfying these growing demands. On the other hand, the optical-time-division multiplexing (OTDM) under research will be one of the anticipative ways for our future backbone systems. The OTDM will be able to realize over-100-GHz ultrafast communication speeds per one fiber, per one wavelength channel, with less power consumptions, with using ultrafast optical clock-pulse generators, and some other ultrafast all-optical devices.

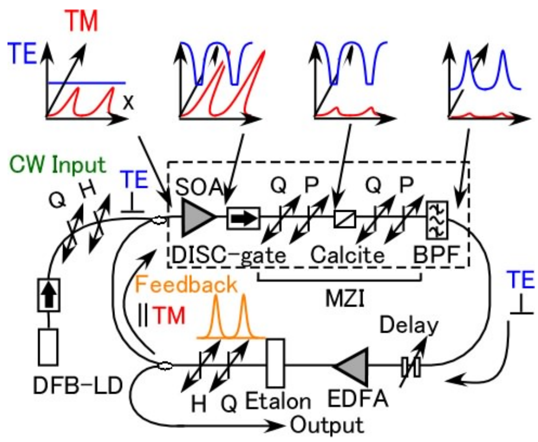

Fig. 1: Schematic view of our DISC-loop-type, optical-clock-pulse generator[5-8]

Regarding the optical-clock-pulse generators for use in the OTDM systems, so-called mode-locked laser diodes (MLLD) which contained ultrafast saturable-absorber (SA) materials had intensively been studied since much 1980's.[4] More recently, a new type of mode-locked semiconductor-laser scheme has been proposed and experimentally demonstrated.[5-8] This laser scheme (i.e., clock-pulse generator) consists of a semiconductor optical amplifier (SOA), some of polarization components, a ring cavity, and an external cw light source, as is schematically shown in Fig. 1. A part of these optical components inside the ring cavity works as an all-optical polarization converter, in a manner similar to the conventional delayed-interference signal-wavelength converters (DISC) under research.[9-11] The polarization directions of the re-circulating optical components are aligned so that any continues-wave (cw) laser oscillation is suppressed in this ring cavity. Since the physical mechanism of this mode-locked pulsed laser oscillation differs from any of conventional mode-locked semiconductor lasers, its new physical mechanism had recently been developed and experimentally verified.[6, 7] Among them, the laser-cavity's threshold gain that is required to start the pulsed laser oscillation was once experimentally studied in Ref. 7. We had not yet, *however*, understood how precisely we must adjust our ring-cavity's polarization components for sufficiently suppressing the cw lasing, and the physical sources of this requirement.

In this paper, we have developed and then experimentally verified a new physical model that explains the preciseness required in this new, mode-locked laser scheme.

2. Working principle of our pulsed laser, from our previous works

In Fig. 1, the rotating processes of the polarization states (either transverse-electric (TE) or transverse-magnetic (TM) modes) of the circulating optical components are schematically indicated, across the ring cavity. The state of the cw component from the external distributed-feedback laser diode (DFB-LD) is aligned to the TE mode inside the SOA by the half- and quarter-wave plates (H and Q). The TE-mode component at the output of the DISC-gate part forms a train of pulses, as is described soon, and then they return to the SOA's input port. In contrast, any orthogonally polarized (i.e., TM-mode) components at the output of the DISC-gate part, which include SOA-amplified pulses, are removed by the polarizer near the output of the DISC-gate part. When the train of pulses returns to the SOA's input port, their polarization state is intentionally adjusted to the TM mode with using the half- and quarter-wave plates located before the output coupler.

When the train of short pulses starts re-circulating inside the ring cavity (Fig. 1), the pulsed laser oscillation stably continues in the following semiconductor-nonlinear-optics manners.[5] When the TE-mode cw component propagates through the nonlinear SOA together with a train of co-propagating TM-mode pulses, the cw component is both cross-phase-modulated (XPM) and cross-gain-modulated (XGM) inside the SOA, and then goes through the asymmetric Mach-Zender interferometer (MZI) whose relative delay time (5 picoseconds) between the two interferometer arms is defined by the birefringence of the high-quality calcite crystal. When the orthogonally polarized (i.e., TM-mode) components are blocked by the polarizer near the output of DISC, the all-optically modulated TE-mode component forms a train of new pulses. The width of these new pulses approximately matches to the interferometer's delay time.[9, 10] In the next step, this train of new pulses resonantly pass through the Fabry-Perot etalon, whose traveling time in its one-round-trip internal reflections was set to either 100 ps (10 GHz) or 25 ps (40 GHz).

In the second next step, the train of new pulses return to the SOA's input port. The new pulses in the TM mode inside the SOA all-optically modulate the co-propagating TE-mode cw component. Thus, we regard this pulse's re-circulation as a *positive feedback loop* of a train of pulses from the output of the DISC gate to its input. The ring-cavity's round-trip frequency (in the order of 10 MHz) must match to one of the sub-harmonic frequencies of the etalon, so that the conventional harmonic mode-locking condition is satisfied.[12]

Obviously, the re-circulating feedback pulses must be strong enough to all-optically modulate the DISC gate and then re-generate strong enough new pulses. For compensating for the relatively large sum of insertion losses of passive optical components including the etalon along our proto-type experimental ring-cavity structure, we are currently using a home-made, low-dispersion Er-doped fiber amplifier (EDFA) inside the cavity (Fig. 1).

The round-trip gain that is required to start the mode-locked pulsed laser oscillation has previously been modeled, as follows,[7]

$$G^{pulse}{}_{loop} = T^{pulse}{}_{DISC} - L_{passive} + G_{EDFA} \text{ (in dB)}. \quad (1)$$

$G^{pulse}{}_{loop}$ is the round-trip gain with respect to the re-circulating pulses. $T^{pulse}{}_{DISC}$ is the transmittance of the all-optical DISC gate, that is, the ratio of the output-pulse's energy to the input-pulse's energy.[7] $L_{passive}$ is the sum of linear insertion losses of all passive optical components (except those inside the DISC gate) after the one round trip. G_{EDFA} is the unsaturated gain of the EDFA. When $G_{loop}>0$, this laser cavity should start generating the pulses. In other words, when $G_{EDFA} > G^{pulse,\ threshold}{}_{EDFA}$, the laser cavity should start generating the pulses. This EDFA's pulse-lasing-threshold gain is defined as,

$$G^{pulse,\ threshold}{}_{EDFA} = L_{passive} - T^{pulse}{}_{DISC} \quad \text{(in dB)} \quad (2)$$

Figure 2 shows measured auto-correlation traces of ultrafast 40-GHz mode-locked pulses from such a ring-laser cavity, in one of our previous works.[7]

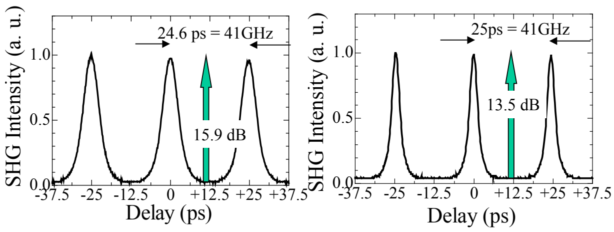

(a) (b)

Fig 2: Measured auto-correlation traces of mode-locked ultrafast pulses,[7] generated by the ring-laser scheme in Fig. 1.
(a) 5-ps, 41-GHz pulses, Δt·Δf= 0.59,
(b) 2.2-ps, 41-GHz pulses, Δt·Δf= 0.53.

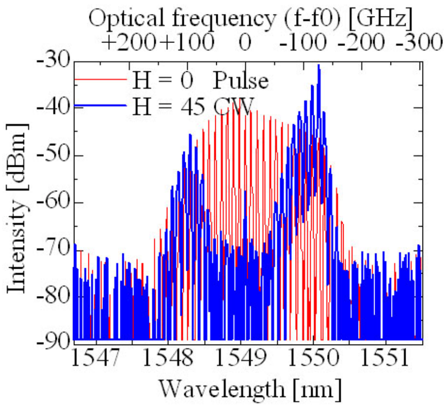

Fig. 3: Contrast between the optical spectra of our mode-locked pulse laser oscillation (red curve) and the unintentional cw laser oscillation (blue curve), depending upon the crystal-axis angle of the half-wave plate inside the laser cavity.

On the other hand, the red curve in Fig. 3 shows one of the optical spectra of our high-quality, mode-locked, 5-ps, 10-GHz, pulsed laser oscillation, measured in this work. The equally spaced optical-frequency distance between the positions of the many line-spectral components matches to the repetition frequency of the pulses. It was 10 GHz in Fig. 2, as a matter of fact. The width of the spectral envelope, in contrast, approximately matches to the Fourier-transform-limited width, taking into account the measured temporal width of the mode-locked pulses.[5-7]

It should be noted here that, when the cw laser oscillation takes place with an EDFA gain level lower than that is required for the pulsed laser oscillation, the pulsed laser oscillation *will never take place* even with a gain level higher than the cw-lasing threshold. It is because the unintentional cw laser component automatically starts strongly saturating the gain of the SOA. The blue curve in Fig. 2 shows a typical optical spectrum of such quasi-cw laser oscillation that was, in fact, completely preventing any pulsed laser oscillation. The blue curve in the figure was measured after temporarily switching the relative angle of the half-wave plate from 0 to 45 degrees so that the cw laser oscillation will take place the most easily, independently from the externally injected 1549-nm cw component. [The externally-injected-cw component is very weakly visible in the blue curve in Fig. 2, separately from the two strong, quasi-cw lasing components.]

Finally, the optical-frequency distance (approximately 200 GHz) between the two noisy quasi-cw lasing peaks in Fig. 2 matched to the distance [$(5\text{ ps})^{-1}$= 200 GHz] between the two adjacent transmission peaks of the MZI with a relative delay time Δt of 5 ps, in the present work. This is because the qusi-cw laser oscillation almost always took place the most easily at the two adjacent optical-transmission-peak positions of the MZI.

3. How precisely we need to suppress unintentional cw lasing for generating pulses

In this work, we first developed a first-order-approximation theoretical model that would explain how precisely we need to suppress the cw lasing, as follows. In contrast to the pulse-lasing model described near Eqs. 1 and 2, we took into account the best condition of the DISC-loop laser cavity for cw lasing. It should be the condition where the first polarizer located between the SOA and calcite does not cut-off any of the cw component that re-circulates from the second polarizer near the output of the DISC gate, through the following quarter-wave and half-wave plates near the output coupler (Fig. 1). The round-trip gain level ($G^{cw}{}_{loop}$) with respect to the unintentionally-and-strongly re-circulating cw-lasing component will be expressed as,

$$G^{cw}{}_{loop} = G_{SOA}(I_{cw}) - L_{DISC} - L_{passive} - L_{pol} + G_{EDFA} \quad (3)$$

$G_{SOA}(I_{CW})$ is the gain of the SOA partially saturated by the externally injected DFB-laser's cw component with an intensity level, I_{cw}. L_{DISC} is the sum of linear insertion losses caused by all passive optical components inside the DISC-gate part. L_{pol} is the linear loss casued by the first polarizer, which is described as,

$$L_{pol} = -10 \log_{10} \sin^2 (2\theta_H) \quad \text{(in dB).} \quad (4)$$

according to the standard Jones-matrix formulae. θ_H is the relative rotational angle of the half-wave plate (which is temporarily detuned from its optimal position, θ_H = 0) The cw laser oscillation will take place immediately when $G^{cw}{}_{loop}$ goes above zero ($G^{cw}{}_{loop} > 0$). This cw-lasing condition is re-written from the viewpoint of the inserted EDFA gain as,

$$G_{EDFA} > G^{cw,\ threshold}{}_{EDFA}, \quad (5)$$

$$G^{cw,\ threshold}{}_{EDFA} = -\ G_{SOA}(I_{cw}) + L_{DISC} + L_{passive} + L_{pol} \quad (6)$$

The best cavity condition where the cw laser oscillation takes place the most easily (i.e., with the lowest EDFA gain level) is described as,

$$\theta_H = 45 \text{ degrees, and,}$$
$$L_{pol} = 0 \text{ dB.} \quad (7)$$

The blue-curve spectrum in Fig. 3 was supposed to be taken under this best condition.

Alternatively, when we try to start pulsed laser oscillation, we switch θ_H from 45 back to nearly 0 degree (Fig. 2). L_{pol} is then increased significantly, following the angle dependence in Eq. 4. So that the pulse laser oscillation starts before the cw laser oscillation starts, the requirement for the pulsed laser oscillation is expressed by the inequality relationship,

$$G^{pulse}{}_{loop} > G^{cw}{}_{loop}, \quad (8)$$

which is obviously equivalent to,

$$G^{pulse,\ threshold}{}_{EDFA} < G^{cw,\ threshold}{}_{EDFA}. \quad (9)$$

Hereafter, we define the EDFA's minimum threshold gain for the quasi-cw lasing, $G^{cw,\ min\ \ threshold}{}_{EDFA}$, as,

$$G^{cw,\ min\ \ threshold}{}_{EDFA} = -\ G_{SOA}(I_{cw}) + L_{DISC} + L_{passive}.$$

$$\tag{10}$$

With using Eqs. 6 and 10, the inequality requirement (9) is re-written as,

$$G^{pulse,\ threshold}_{EDFA} < G^{cw,\ min.\ threshold}_{EDFA} + L_{pol}. \tag{11}$$

Now we reach the inequality requirement which the loss L_{pol} needs to satisfy,

$$L_{pol} > L^{min}_{pol} \tag{12}$$

where the required minimum loss, L^{min}_{pol}, matches to the relative distance between the two completely alternative types of threshold gains as,

$$L^{min}_{pol} = \Delta G^{threshold}_{EDFA}, \text{ and,} \tag{13}$$

$$\Delta G^{threshold}_{EDFA} = G^{pulse,\ threshold}_{EDFA} - G^{cw,\ min.\ threshold}_{EDFA}. \tag{14}$$

Using the definitions in Eqs. 2 and 6, the threshold-gain distance is expressed as,

$$\Delta G^{threshold}_{EDFA} = -T^{pulse}_{DISC} + G_{SOA}(I_{cw}) - L_{DISC}. \tag{15}$$

To summarize, the inequality requirement (12) directly tells us how strongly we need to suppress the unintentional quasi-cw laser oscillation with precisely adjusting the polarization state of the propagating optical component (i.e., with precisely adjusting the rotational angle θ_H of the half-wave plate inside the ring cavity). According to the following Eqs. 13-15, the physical factors that define the preciseness required in our semiconductor-laser cavity scheme have turned out to be the following three factors, the transmittance T^{pulse}_{DISC}, the gain $G_{SOA}(I_{cw})$, and the loss L_{DISC}. It should be noted that the required preciseness is inherently independent from the EDFA gain which is added for compensating for linear insertion losses. All of the three physical factors are originated from optical components inside the all-optical DISC-gate part.

4. Experimental evidences

We tried to experimentally verify the new model in the previous section in the following three steps. In the first step, we studied the threshold-gain's distance, $\Delta G^{threshold}_{EDFA}$ in Eq. 14, for the first time. Figure 4 shows the measured ring-cavity's output power as a function of the relative gain parameter,

$$\Delta G_{loop} = G_{EDFA} - G^{pulse,\ threshold}_{EDFA} \quad \text{(in dB)}. \tag{16}$$

When θ_H was carefully adjusted to the optimum direction (i.e., 0 degree by the definition of θ_H), the pulsed laser oscillation started right after the relative gain approximately exceeded 0 dB.[6] This fact is consistent with our definition of $G^{pulse,\ threshold}_{EDFA}$.

When θ_H was switched from 0 to 45 degrees, the cw laser oscillation instead started with much smaller EDFA gains. In case of our laser cavity with a 10-GHz etalon, 20dB-less EDFA gain was required for its quasi-cw lasing. In case of that with a 40-GHz etalon, 17dB-less EDFA gain was required. In other words, the threshold positions in the relative loop gain ΔG_{loop} were measured to be -20dB and -17dB, respectively, for the cw lasing in the 10-GHz cavity and that in the 40-GHz cavity (Fig. 4). As was described in the previous section, we are believing that these amounts of threshold-gain's distances, $\Delta G^{threshold}_{EDFA}$ are specifically indicating to which extent we need to suppress the unintentional cw lasing before the pulse laser oscillation takes place in these laser cavities.

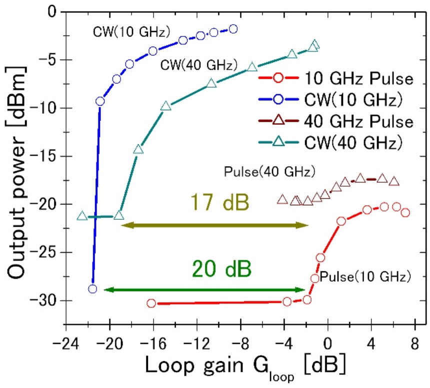

Fig. 4: Measured ring-cavity's output power as a function of the relative loop gain, ΔG_{loop}, which is defined by Eq. 16 in the text.
The half-wave-plate angle θ_H was set to either 0 degree (for pulsed laser oscillation) or to 45 degrees (for quasi-cw laser oscillation). Both of the 10-GHz cavity and the 40-GHz cavity were systematically tested.

In the second step, we more systematically investigated the threshold-gain positions for the cw laser oscillation, as a function of the wave-plate angle, θ_H. Figure 5 shows the measured threshold-EDFA gains. In addition, the dashed curves show the calculated threshold gains, with relying upon Eq. 4. From the viewpoint of these threshold gains, the behavior of the quasi-cw laser oscillation has matched well with our new model described in the previous section.

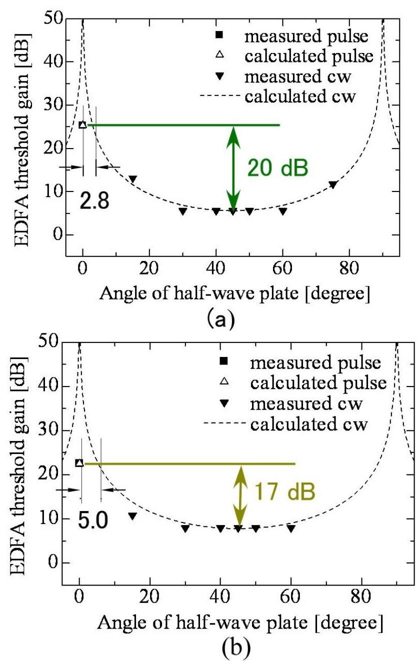

Fig. 5: Threshold-EDFA gains for the pulse laser oscillation and those for the quasi-cw laser oscillation, systematically measured as a function of the half-wave plate angle , θ_H.
(a) with the 10-GHz cavity, (b) with the 40-GHz cavity.

In the third step, we finally paid attention to the *preciseness* required in adjusting the stateof the polarization, from the viewpoint of the polarization-controlling wave-plate angle, θ_H. By combining the calculated results with the measured results in Fig. 5, we speculated that the threshold gain for the cw-lasing would go above that for pulse-lasing (as was described in Eq. 9), when θ_H reaches less than 2.8 degrees (Fig. 5(a)) and 5.0 degrees (Fig. 5(b)), respectively. It means that the pulse laser oscillation will take place, only when θ_H is adjusted precisely enough within the above-mentioned finite angle range between -2.8 degrees and +2.8 degrees (in case of Fig. 5(a)).

Independently from these speculations about the angle θ_H's preciseness requirement, we experimentally characterized this preciseness requirement. In the experimental characterization, we tried to hold one of the successful pulse laser oscillation, by intentionally, carefully, and slowly detuning θ_H from its optimal position, right after our precisely optimizing θ_H for high-quality pulse laser oscillation. The widths of the acceptable θ_H range measured in this manner from December 2007 through January 2008 were ±3 degrees with the 5-ps, 10-GHz cavity, and ±5 degrees with the 5-ps, 40-GHz cavity, respectively. [In these experiments, all pigtail fibers and other connection fibers inside the cavity were very carefully stabilized to the surface of our optical bench with using conventional Scotch tapes, so that the states of polarization would be stabilized precisely enough.] As a consequence, the experimentally measured widths of the acceptable θ_H range have matched well with those speculated from the earlier-mentioned results in Fig. 5.

5. Conclusion

After the series of our previous experimental works (Fig. 2 and Refs. 5-8) regarding this original semiconductor-laser cavity scheme, we paid the very first attention to the required preciseness in this laser scheme's critical adjustment, that is, how precisely we need to suppress unintentional quasi-cw lasing for start generating the 5-ps, 40-GHz optical clock pulses. In general, the lower the minimum threshold gain for the quasi-cw lasing is, the more precisely-and-strongly we need to suppress the cw lasing.

In the first step, we expanded our theoretical model (Eqs. 1 and 2) for taking into account the unintentional cw laser oscillation (Eq. 3), and then analytically derived the inequality requirement (12), under whose condition the pulse laser oscillation will take place before the quasi-cw laser oscillation starts saturating the nonlinear SOA, i.e., the driver component inside the all-optical DISC gate. In the next step, we experimentally characterized the required preciseness in the adjustment of one of the most critical cavity components, i.e, one of the polarization-controlling components. Up to now, our systematically measured widths of acceptable adjustment range (±5 degrees in case of our 5-ps, 40-GHz laser cavity or ±3 degrees in case of our 5-ps, 10-GHz laser cavity) have matched fairly well with those calculated from our new model.

According to the above-mentioned new model of ours, the physical factors that define the required preciseness have turned out to be the following three factors, the transmittance T^{pulse}_{DISC}, the gain $G_{SOA}(I_{cw})$, and the loss L_{DISC}. All of these physical factors are originated from the all-optical DISC-gate part in Fig. 1. We believe these results and conclusions in this work will be extremely valuable, both for up-grading the optical-clock-pulse's width generated by this laser scheme to less than one picosecond and for upgrading its repetition frequency to 100-to-300GHz regions. They will be very valuable, as well, for our start monolithically integrating some hundreds of these clock-pulse generators and their families on the surface of a III-V semiconductor chip, without requesting too much precision in the nano-fabrication processes. The required preciseness of ±5 degrees in terms of an optical component's rotational angle, required in this first research work as an example, will not be a big burden in the *volume-production-level nano-semiconductor-fabrication processes*.

References

1. OECD Broadband Portal, http://www.oecd.org/sti/ict/broadband/
2. OECD Broadband Statistics, December 2004, http://www.oecd.org/document/60/0,3343,en_2825_499582_2496764_1_1_1_1,00.html
3. China Statistical Yearbook 2007, http://www.stats.gov.cn/tjsj/ndsj/2007/indexeh.htm
4. e.g.: K. Sato, "Semiconductor light sources for 40-Gb/s transmission systems," J. Lightwave Technol., Vol. 20, No.12, pp. 2035-2043, 2002.
5. Yoshiyasu Ueno, Shigeru Nakamura, and Kazuhito Tajima, "5-ps, 10-GHz pulse generation from an all-optical semiconductor switch embedded in a ring cavity," Appl. Phys. Lett., Vol. 79, No. 16, pp. 2520-2522, 2001.
6. Rei Suzuki, Satoshi Kobayashi, Jun Sakaguchi, and Yoshiyasu Ueno, "Threshold condition for pulse generation from a DISC-loop-type pulse generator," IQEC/CLEO-PR, CFM1-4 2005.
7. Rei Suzuki, Takashi Ohira, Jun Sakaguchi, and Yoshiyasu Ueno, '40-GHz mode-locked pulse generation with a new scheme of SOA-based pulse generation,' CLEO/QELS 2006, May 21-26, 2006, Long beach, USA, paper no. CMG5.

8. Ryoichi Nakamoto, Hiroyuki Takeuchi, Jun Sakaguchi, and Yoshiyasu Ueno, "1.55-um, mode-locked, single-longitudinal-mode, 10-GHz, 2-ps, ultra-short optical pulse train from our original semiconductor-based pulse-source scheme," Topical Conference on Nanophotonics (NANO), Optical Society of America, May 26-29, 2008, Southeast Univ., Nanjing, P.R. China, paper no. Nano-08-191.
9. Y. Ueno, S. Nakamura, K. Tajima, and S. Kitamura, "3.8-THz wavelength conversion of picosecond pulses using a semiconductor delayed-interference signal-wavelength converter (DISC)," IEEE Photonics Technol. Lett. vol. 10, no. 3, pp. 346-348, March 1998.
10. Y. Ueno, S. Nakamura, and K. Tajima, 'Nonlinear phase shifts induced by semiconductor optical amplifiers with control pulses at repetition frequencies in the 40-160 GHz range for use in ultrahigh-speed all-optical signal processing,' J. Opt. Soc. Am. vol. B19, no. 11, pp. 2573-2589, Nov. 2002.
11. Jun Sakaguchi, Ferran Salleras, Kohsuke Nishimura, and Yoshiyasu Ueno, "Frequency-dependent electric dc power consumption model including quantum-conversion efficiencies in ultrafast all-optical semiconductor gates," Optics Express vol. 15, no. 22, pp. 14887-14900, Oct. 2007.
12. e.g.: C.M. DePriest, T. Yilmaz, P. J. Delfyett, Jr., S. Etemad, A. Braun, and J. Abeles, ”Ultralow noise and supermode suppression in an actively mode-locked external-cavity semiconductor diode ring laser,” Opt. Lett., Vol. 27, No. 9, pp.719-721, 2002.